EasyChair Preprint

№ 5160

Experimental Observations and Data Analysis of a Commercially Grade Aluminium Alloy (6082T6) for Large Elasto Plastic Deformation

Venkatesh Donekal, K R Phaneesh, Pradeep K V Kumar, S V Prakash, Arun R Rao and Shrinivasa Udipi

March 16, 2021

Experimental observations and data analysis of a commercially grade Aluminium alloy (6082T6) for large elastoplastic deformation

D. Venkatesh[1], K. R. Phaneesh[2], Pradeep Kumar K. V.[3]
S.V.Prakash[4], Arun R. Rao[5] Udipi Shrinivasa[6]

[1,2,3]Department of Mechanical Engineering, M.S. Ramaiah Institute of Technology, Bangalore-560003
[4]Sri Krishna Institute of Technology, Bangalore-560090
[5,6]Department of Mechanical Engineering, Indian Institute of Science, Bangalore-560001
[1]D. Venkatesh – venkatesh@msrit.edu - Corresponding Author

Abstract:

Large elastoplastic deformation generally occurs in sheet-metal forming processes during stretching, blanking, punching, stamping, bending, bending-unbending, reverse bending and deep drawing. In today's world, due to very high competition and swift development of products in metal forming industries, there is a growing demand in high precision end products to be manufactured in short duration. It is very essential and important to have a knowledge of an in-depth understanding of material behaviour in all these metal forming steps. Therefore, to predict material behaviour, an accurate material modelling is required by considering the simultaneous effects of strain and strain rate. Classical flow rules are generally used to predict the material behaviour in the post yield range. Overall material deformation can be represented as the change in size, change in shape and their rates. A new generalised relation is developed to represent the material behaviour from elastic range to failure. This relation involves eight material parameters which includes two classical material constants like bulk modulus and shear modulus, two material viscosity terms and four in the form rule which relates elastic strain rate to plastic strain rate. All these material parameters can be obtained from uniaxial tension experiments. The material deformation is 3-D in nature and therefore classical yield criteria is avoided while formulating the relation. Instead, concept of activation energy is used. In the present work, experimental observations and data analysis on the commercial grade aluminium (6082T6) was discussed. The material behavior in the post yield region with new understanding of the material model was presented here for uni-axial loading case. Based on the experimental observations and the results obtained it was found that the both the elastic moduli and the viscosities remain constant throughout the large deformation.

Keywords: Sheet metal forming, material model, material constants, strain rate effects, flow rule.

1. Introduction

Sheet metal forming is one of the most widely used material-processing operations in many applications especially in automobile industries. Stretch forming process is frequently employed in automotive sector to manufacture complex and intricate shaped parts like outer panels, inner panels, stiffeners etc. Besides most of the metal forming operations finds use in the packaging industry and in the household appliances sector to manufacture complicated shapes and curvatures. It is common phenomenon where a piece of material is plastically deformed between tools to obtain the desired shape. In order to replace presently used trial and error method, accurate prediction of tool geometries and manufacturing parameters are essential. Certain defects like local thinning, wrinkling, tearing, shear fracture, buckling, shape distortion, loose metal and undesirable surface textures or defects etc. associated with metal forming operations are eliminated by simulation tools which require field equations from first principles. Prediction of spring back requires a thorough understanding of deformation mechanics and material behavior in the plastic range. Material essentially deforms in both elastic and plastic ranges in the stretch forming operation. The generalized Hook's law is used to express the linear trend of infinitesimal deformation during the elastic behavior of material based on the classical theory. The macroscopic behavior of metals in the uniform state of combined stresses is developed to explain the plasticity theory is based on certain experimental observations. Macroscopic models are preferred over microscopic models in terms of cost and computational time. Also overall deformation can be represented very easily through macroscopic behavior. Traditionally, large elastoplastic deformation theory is based on classical yield theories which do not accurately predict the material behavior, spring back and other parameters required for die design, tooling and metal working industries.

To describe the complex behavior of metals under combined state of stresses, experimentally observed results are idealized into mathematical formulations. These formulations are obtained based on certain assumptions like material behavior is time independent, i.e. strain rate effects are neglected, hysteresis loop and Bauschinger effects which arise from the non-uniformity of the microscopic scale are disregarded etc. The thermal effects are neglected and the material is assumed to be isotropic. Hence in order to develop and validate unified constitutive model for large elasto plastic deformation, it is essential to understand the material behavior and physics behind the plastic

deformation behavior. Also it is required to carry out uni-axial and bi-axial tension and compression experiments for measurements and data analysis for accurate prediction of material deformation behavior. For model verification and prediction, numerous efficient numerical simulation techniques and tools need to be developed. The mechanical properties such as elasticity, plasticity, ductility, yielding, creep, fatigue etc. depends on strain, strain rates, temperature during loading and unloading. Therefore, all the manufacturing and material processes such as metal forming, high speed machining, high velocity impact, penetration mechanics and other static and dynamic loading conditions etc, requires an in depth understanding of material behavior due to temperature and strain rates. In the design of structure, machining tools and processes, all the parameters like strain rate and temperature dependence need to be taken into account.

The aim of this research is to develop an experimental model to represent the material behavior from elastic range to failure. Experimental tests were performed to predict deformations in loaded materials under elastoplastic deformations and compare the theoretical results with experimental observations in the laboratory. This relation involves eight material parameters which includes two classical material constants like bulk modulus and shear modulus, two material viscosity terms and four in the form rule which relates elastic strain rate to plastic strain rate. All these material parameters can be obtained from simple experiments. The main purpose of this experimental model is to represent the three dimensional nature of stress-strain behavior in the elastic range, transition from elastic to plastic state and also in the plastic range with minimum number of deformation parameters. The material deformation is 3-D in nature and therefore classical yield criteria is avoided while formulating the relation. Instead, concept of activation energy is used. Experiments were carried out to find material parameter values. In the present work, experiments on the commercial grade aluminum was discussed. The model was based on a generalized macroscopic theory, taking into account experimental test data and microscopic understanding of material deformation. The material deformation is considered as the continuous contribution from strain and strain rate part while inelasticity is always present under all kinds of loading.

The main purpose of this work is to understand the behavior of elastic modulus of metals in terms of volumetric and shear components, for large elastoplastic deformation. Also to determine two more material parameters like material shear viscosity due to deviatoric strain rate part and material bulk viscosity due to volumetric strain rate part for inelastic deformation, exhaustive experimental measurements and data analysis were carried out. The experimental model presented here is to get insight into the material behavior under varying strain rates and various loading conditions.

2. Problem Formulation

2.1 Field equation

The new field equation consists of elastic resistance from strain and dissipative force which arises from strain rate. The stress relation for a material during deformation can be expressed as

$$\sigma = \sigma_e + \sigma_p \tag{2.1}$$

The first term σ_e in equation 2.1 is associated with the elastic strain part while the next term σ_p, (viscous stress) is associated with plastic strain rate. Expressing these in the form of change in size, change in shape and their rate terms,

$$\sigma_e = K(\acute{\varepsilon}_1 + \acute{\varepsilon}_2 + \acute{\varepsilon}_3)I + 2G\left(\begin{bmatrix} \acute{\varepsilon}_1 & 0 & 0 \\ 0 & \acute{\varepsilon}_2 & 0 \\ 0 & 0 & \acute{\varepsilon}_3 \end{bmatrix} - \frac{(\acute{\varepsilon}_1+\acute{\varepsilon}_2+\acute{\varepsilon}_3)}{3} I\right) \tag{2.2}$$

$$\sigma_p = \mu' \frac{\partial}{\partial t}(\acute{\varepsilon}_1 + \acute{\varepsilon}_2 + \acute{\varepsilon}_3)I + 2\mu \frac{\partial}{\partial t}\left(\begin{bmatrix} \acute{\varepsilon}_1 & 0 & 0 \\ 0 & \acute{\varepsilon}_2 & 0 \\ 0 & 0 & \acute{\varepsilon}_3 \end{bmatrix} - \frac{(\acute{\varepsilon}_1+\acute{\varepsilon}_2+\acute{\varepsilon}_3)}{3} I\right) \tag{2.3}$$

$$\sigma_e = K\Theta_e I + 2G\left(\varepsilon_e - \frac{\Theta_e}{3} I\right) \tag{2.4}$$

$$\sigma_p = \mu'\dot{\Theta}_p I + 2\mu\left(\dot{\varepsilon}_p - \frac{\dot{\Theta}_p}{3} I\right) \tag{2.5}$$

Where K and G are elastic constants known as bulk and shear modulus respectively. μ and μ' are material viscosities known as material bulk viscosity and material shear viscosity respectively. ε is the component of normal strain and Θ represents the cubical dilatation (Volumetric strain). ε_e and ε_p denote the strains associated with elastic and plastic strains respectively. $\dot{\varepsilon}_e$ and $\dot{\varepsilon}_p$ denotes the corresponding elastic and plastic strain rate. Now substituting the contribution from the strain and strain rate parts in equation 2.1 we get,

$$\sigma = K\Theta_e I + 2G\left(\varepsilon_e - \frac{\Theta_e}{3} I\right) + \mu' \dot{\Theta}_p I + 2\mu\left(\dot{\varepsilon}_p - \frac{\dot{\Theta}_p}{3} I\right) \tag{2.6}$$

$$\sigma = K(\Theta_e) I + 2G\left(\varepsilon_e - \frac{\Theta_e}{3} I\right) + \mu' \frac{\partial}{\partial t}(\Theta_p) I + 2\mu \frac{\partial}{\partial t}\left(\varepsilon_p - \frac{\Theta_p}{3} I\right) \tag{2.7}$$

Where Θ_e and Θ_p are the elastic and plastic parts of the volumetric strain respectively. In Eqn. 2.7, elastic moduli, K and G are constants associated with the elastic volumetric and the elastic deviatoric strains respectively. The other two material parameters, material viscosities μ *and* μ', are also constants and associated with the plastic strain rate part. The plastic parts of the volumetric and deviatoric strains have appeared only as strain rates. These plastic parts represent the energy loss in the form of dissipation during deformation. Since plastic strains are due to inter crystalline activities and plastic strain rates are functions of the corresponding elastic strain and strain rates, the relation between the plastic strain rate and elastic strain rate for volumetric and deviatoric components can be expressed as

$$\dot{\Theta}_p = \phi(\Theta_e, \dot{\Theta}_e)\, \dot{\Theta}_e \tag{2.8}$$

$$\dot{\varepsilon}_{dp} = \psi(\mathrm{J}_{2e}, j_{2e})\, \dot{\varepsilon}_{de} \tag{2.9}$$

Where $\dot{\Theta}_p$, $\dot{\varepsilon}_{dp}$, $\dot{\Theta}_e$ and $\dot{\varepsilon}_{de}$ are the hydrostatic and deviatoric components of the plastic and elastic strain rate tensor respectively. ϕ and ψ are material parameters and vary with deformation. Φ is a function of elastic volumetric strain, Θ_e and its rate $\dot{\Theta}_e$. Similarly, ψ is the function of second variant of the deviatoric elastic strain tensor, J_{2e}, and its rate j_{2e}.

The stress-strain relation in Eqn. 2.7 needs only the gradient of σ to represent the material deformation. In the literature, some of the authors like Zener and Hollomon [72] in the year 1946, Lazan [45] in the year 1968 believed that no real metal possesses an ideally elastic region and material deformation is due to continuous contribution from elastic and plastic parts. That is, even at very low stresses, inelasticity is always present under all types of loading. Therefore, while considering material deformation, elastic and plastic effects should be taken into effect. This criteria avoids any assumption of yield condition or yield surfaces to determine any elastic-plastic boundary, which may not exist according to Seth, 1970 [58]. The above Eqn. holds fairly well with these observations.

The above formulation consists of eight material parameters. Out of these, two are associated with elastic deformation, bulk modulus (K) and shear modulus (G), the other two are associated with viscous deformation, material bulk viscosity (μ') and material shear viscosity (μ), while the remaining four constants are activation points associated with hydrostatic strain (θ_y), and deviatoric strain (J_{2y}) and the corresponding plastic strain rates (ϕ) and (ψ). All these constants are obtainable from uniaxial tension experiments. However in order to predict the elastoplastic deformation accurately and investigate the new theory as proposed by Rao [54] in the year 2007 and Jain. P [36] in the year 2006, it is required to measure strains in all three directions and three dimensional stress-strain behaviours of materials in the entire stress-strain range. This can be predicted based on uniaxial tension test.

2.2 Determination of material parameters

From experiments, the basic data available are, applied load, axial and lateral strains as functions of time and at varying strain rates. The values of material parameters, K, G , μ, μ' appearing in equation 2.7 can be determined using uni axial tension experiments at small strains and strain rates. At higher strain and strain rates, these constants are affected by material non-linearities. During uniaxial tension test, the applied stress in the lateral direction is zero. i.e., $\sigma_2 = \sigma_3 = 0$. Therefore the new field eqn. takes the form;

$$\sigma_1 = K(\varepsilon_{1e} + \varepsilon_{2e} + \varepsilon_{3e}) + 2G\left(\varepsilon_{1e} - \frac{\varepsilon_{1e}+\varepsilon_{2e}+\varepsilon_{3e}}{3}\right) + \mu'(\dot{\varepsilon}_{1p} + \dot{\varepsilon}_{2p} + \dot{\varepsilon}_{3p}) + 2\mu\left(\dot{\varepsilon}_{1p} - \frac{\dot{\varepsilon}_{1p}+\dot{\varepsilon}_{2p}+\dot{\varepsilon}_{3p}}{3}\right) \tag{2.10}$$

$$0 = K(\varepsilon_{1e} + \varepsilon_{2e} + \varepsilon_{3e}) + 2G\left(\varepsilon_{2e} - \frac{\varepsilon_{1e}+\varepsilon_{2e}+\varepsilon_{3e}}{3}\right) + \mu'(\acute{\varepsilon}_{1p} + \acute{\varepsilon}_{2p} + \acute{\varepsilon}_{3p}) + 2\mu\left(\acute{\varepsilon}_{2p} - \frac{\acute{\varepsilon}_{1p}+\acute{\varepsilon}_{2p}+\acute{\varepsilon}_{3p}}{3}\right) \quad (2.11)$$

$$0 = K(\varepsilon_{1e} + \varepsilon_{2e} + \varepsilon_{3e}) + 2G\left(\varepsilon_{3e} - \frac{\varepsilon_{1e}+\varepsilon_{2e}+\varepsilon_{3e}}{3}\right) + \mu'(\acute{\varepsilon}_{1p} + \acute{\varepsilon}_{2p} + \acute{\varepsilon}_{3p}) + 2\mu\left(\acute{\varepsilon}_{3p} - \frac{\acute{\varepsilon}_{1p}+\acute{\varepsilon}_{2p}+\acute{\varepsilon}_{3p}}{3}\right) \quad (2.12)$$

Where $\acute{\varepsilon}_{1p}$, $\acute{\varepsilon}_{2p}$, $\acute{\varepsilon}_{3p}$ are the rate of plastic strain component and expressed as

$$\varepsilon'_{1p} = (d/dt)\varepsilon_{1p} \; ; \; \varepsilon'_{2p} = (d/dt)\varepsilon_{2p} \; ; \; \varepsilon'_{3p} = (d/dt)\varepsilon_{3p} \quad (2.13)$$

There are three equations and six unknown quantities ε_{1e}, ε_{2e}, ε_{3e}, ε_{1p}, ε_{2p}, ε_{3p} in the form of strain field provided the material constants, K, G, μ', μ are known to solve the system. The plastic strains can be expressed as the difference between total strain and elastic strain.

$$\varepsilon_{1p} = \varepsilon_1 - \varepsilon_{1e} \; ; \; \varepsilon_{2p} = \varepsilon_2 - \varepsilon_{2e} \; ; \; \varepsilon_{3p} = \varepsilon_3 - \varepsilon_{3e} \quad (2.14)$$

The total strains ε_1, ε_2, ε_3 along the three directions, axial and along the width and thickness were measured from uni - axial tension tests. The elastic strains ε_{1e}, ε_{2e}, and ε_{3e} along the three directions were obtained from the tensile test data. Then the corresponding plastic strains ε_{1p}, ε_{2p} and ε_{3p} were calculated from the equation 2.14. The rate of plastic strain components ε'_{1p}, ε'_{2p} , ε'_{3p} were determined with respect to the time for different strain rates from equation 2.13.

Now the equations 2.10 to 2.12 have three unknown quantities in the form of three elastic strains in three directions and three equations to solve the system. Hence the material parameters used in the field equation can be calculated. The elastic constants K and G are obtained by using the classical relation,

$$K = \frac{\sigma_1}{3(\varepsilon_1 - 2\varepsilon_2)} \quad (2.15)$$

$$G = \frac{\sigma_1}{2(\varepsilon_1 + \varepsilon_2)} \quad (2.16)$$

In the above relation, a few initial values of stress and strain are used so that it will be well within the elastic limit and free from any nonlinear effects. Similarly the values for bulk and shear viscosity (μ' and μ) are obtained corresponding to experimental data for aluminium. Next the plastic strains are expressed as the difference between total strain and elastic strain. Thus the whole equation is in terms of total and elastic strains and their rates. The system is solved for elastic strains using the known values of applied stress, total strains in axial and lateral directions and the rate at which these experiments are carried out. Now by knowing the elastic strains, plastic strain and plastic strain rates are calculated. Theoretical and experimentally observed behaviours of material parameters such as bulk modulus (K), shear modulus (G), bulk viscosity (μ), shear viscosity (μ), the ratio of lateral strain (width) to axial strain, i.e. Poison's ratio (ν_1), the ratio of lateral strain (thickness) to axial strain, i.e. Poison's ratio (ν_2), in the existing literature are summarized here. These will then become reference for comparison for the parameters that are going to be computed in this work.

The average Young's modulus E computed for different strain rates using one point, three point, five point, seven point moving point average method. Then the elastic constants K and G were obtained for aluminium. Similarly the average poison's ratio ν_1 and $\nu 2$ can be computed for the aluminium specimen. The standard deviations for aluminium were obtained for various samples are comparatively very small. Finally the values of bulk viscosity and shear viscosity (μ' and μ) are obtained for aluminium specimens.

3. Experimental Observations and Data Analysis

In the present work commercial grade Aluminum alloy (6082T6) was tested using uni-axial tension loading and unloading test. The behavior of material parameters for the new field equation was predicted. Aluminum samples of dimensions measured within +/- 0.05 mm were tested on a strain rate controlled hydraulic tensile testing machine (160 KN capacity) fitted with computer aided automatic data acquisition system to collect load and strain data at BANGALORE INTEGRATED SYSTEM SOLUTIONS (BISS LABS), Bangalore. Load was applied in axial direction within +/- 0.001KN and strain was measured using axial extensometers within +/- 0.001mm in three principal directions, i.e. axial, lateral and across the thickness of the specimen. Strain rates in our measurements were kept between 1E-04 to 1.7E-03 per second (100 μ Strains to 1700 μ Strains). The experimental set up is as shown in Fig. 3.1.

Fig.3.1 Experimental Setup with specimen

3.1 Aluminium specimen

Commercial grade aluminium alloy 6082 T6 samples were chosen for the uniaxial tension experiments. Aluminium alloy is a medium strength structural alloy with excellent corrosion resistance. Among the 6000 series alloys, it has the highest strength. Aluminium alloy is most commonly used for machining in plate form. In many applications, the higher strength of 6082 new alloy replaces 6061 alloy. The addition of a large amount of manganese controls the grain structure which in turn results in a stronger alloy. Aluminium is structurally different than the mild steel. In aluminium, the strain hardening behaviour is not as pronounced as in mild steel and it does not exhibit the upper and lower yield point phenomena observed in mild steel. Also aluminium does not have the transition zone, i.e. increase in strain at a constant load after the yield point which is a characteristic feature of mild steel stress-strain curve. Of late aluminium alloy sheet finds as a replacement for mild steel in automotive bodies due to its higher strength to weight ratio and therefore aluminium is chosen as another material for this study. Commercial grade aluminium is chosen for this purpose. The chemical composition of aluminium conforms to ASTM E 1251-2007. Hardness of the material is tested as per IS 1500-2005 and average Brinell hardness of the material is 96.1.

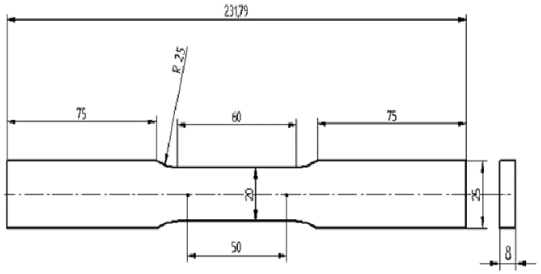

Fig. 3.2. Aluminium specimen Dimensions as per ASTM 8/E 8M-08.

Table 3.1 Dimensions of the test specimen

Parameter	Dimension (mm)
Gage length	50
Width	20
Radius of fillet	25
Overall length	231.79
Length of reduced section	60
Length of the grip section	75
Width of the grip section	25

3.2. Measurement of Material Constants

The cumulative average Young's Modulus (E) Using 1Point, 3 Point, 5 Point and 7 Point moving average method tabulated for all the aluminium specimens (AL_01 to AL_25) for Strain Rates from 0.0001S^{-1} to 0.0017 S^{-1} and is shown in Table 3.2. The cumulative average Young's Modulus (E) is found to be **70697.05 MPa.** The cumulative average Poison's Ratio (ν_1) using 1Point, 3 Point, 5 Point and 7 Point moving average method tabulated for all the aluminium specimens (AL_01 to AL_25) for Strain Rates from 0.0001S^{-1} to 0.0017 S^{-1} is shown in Table 3.3. The cumulative average Poison's Ratio (ν_1) is found to be **-0.32309.** The cumulative average Poison's Ratio (ν_2) using 1Point, 3 Point, 5 Point and 7 Point moving average method tabulated for all the aluminium specimens (AL_01 to AL_25) for Strain Rates from 0.0001S^{-1} to 0.0017 S^{-1} is shown in Table 3.4. The cumulative Poison's Ratio (ν_2) is found to be **-0.32396.**

Table 3.2: Average Young's Modulus (E) Using 1Point, 3 Point, 5 Point and 7 Point (AL_01 to AL_25 Specimens-Strain Rate - 0.0001S^{-1} to 0.0017 S^{-1})

Sl. No.	Method	Average Young's Modulus, E (MPa)
1	First Method (1 Pt. Average)	70786.25
2	Second Method (3 Pt. Average)	70659.13
3	Second Method (5 Pt. Average)	70639
4	Second Method (7 Pt. Average)	70703.82
Cumulative Average Young's Modulus, E (MPa)		**70697.05**

Table 3.3: Average Poison's Ratio (v_1) Using 1Point, 3 Point, 5 Point and 7 Point (AL_01 to AL_25 Specimens- Strain Rate - 0.0001S^{-1} to 0.0017 S^{-1})

Sl. No.	Method	Average Poisson's Ratio (v_1)
1	First Method (1 Pt. Average)	-0.3252
2	Second Method (3 Pt. Average)	-0.32353
3	Second Method (5 Pt. Average)	-0.32634
4	Second Method (7 Pt. Average)	-0.31728
Cumulative Average Poisson's Ratio (v_1)		**-0.32309**

Table 3.4: Average Poison's Ratio (v_2) Using 1Point, 3 Point, 5 Point and 7 Point (AL_01 to AL_25 Specimens- Strain Rate - 0.0001S^{-1} to 0.0017 S^{-1})

Sl. No.	Method	Average Poisson's Ratio (v_2)
1	First Method (1 Pt. Average)	-8.08557
2	Second Method (3 Pt. Average)	-8.03636
3	Second Method (5 Pt. Average)	-8.12712
4	Second Method (7 Pt. Average)	-8.14714
Cumulative Average Poisson's Ratio (v_2)		**-0.32396**

4 Results & Discussion

4.1 Experimental Data Analysis

The Stress v/s strains curves obtained from experimentally available data for commercially available aluminium alloy (6082T6) specimen at different strain rates 100 µstrains and 300 µstrains from loading till failure are shown in graphs Fig. 4.1 and Fig. 4.2. All analysis were carried out on these set of experimental data. For aluminium specimens, the graphs indicates the same value of elongation (>15%) at different strain rates varying from 100 µstrains to 1700 µstrains from loading till failure.

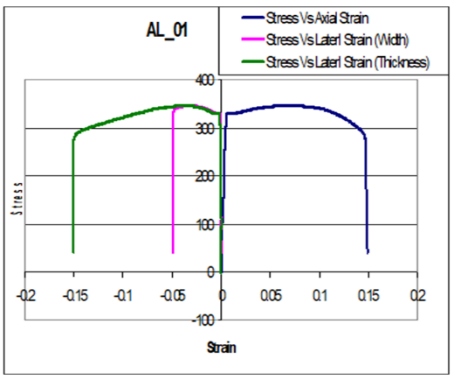

Fig. 4.1. Stress v/s strain curves for aluminium (6082 T6) strained at 100 µstrains

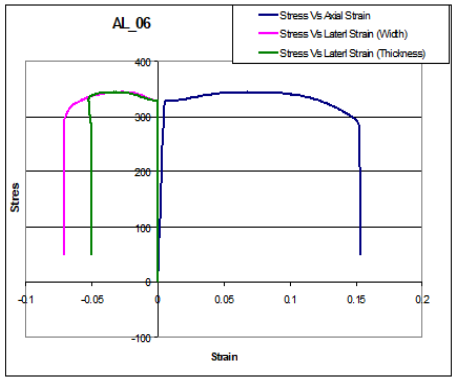

Fig. 4.2. Stress v/s strain curves for aluminium (6082 T6) strained at 300 µstrains

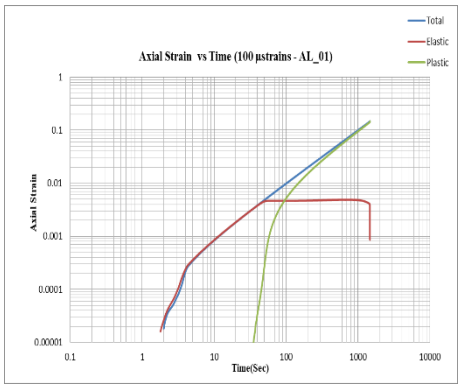

Fig. 4.3 Axial Strain v/s Time

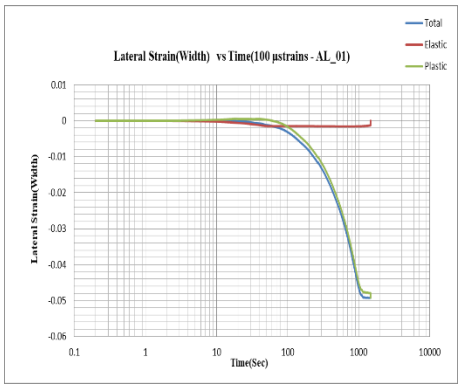

Fig. 4.4 Lateral Strain (width) vs Time

The total axial strains along length, total lateral strains along width and thickness, axial and plastic strains along length, width and thickness are computed for all the strain rates ranging from 100 µstrains to 1700 µstrains for all the Aluminium specimens (AL_01 to AL_25). The contribution from the axial elastic and plastic strain on total axial strain for mild steel strained at 100 µstrains is shown in Fig. 4.3 while, Fig. 4.4 shows for the lateral strains along width and Fig. 4.5 shows for the lateral strain along thickness. In the elastic or earlier part of the deformation region, most of the contribution for total strain comes from elastic strain. In this region, plastic strains are very small or nearly zero. During the latter part of deformation, the contribution from the elastic strain is very less and total contribution remains constant as observed in graphs. After yielding, plastic strain contributes more to the total strain. Major part of the total strain consists of only of plastic strain. The plastic strain rate part contributes very less to the total stress and the major contribution for stress comes from the elastic strain part. The elastic strain is more in aluminium than mild steel indicating mild steel is stiffer than aluminium. Similarly all the above graphs both for aluminium at 300 µstrains, are presented as shown in the Figures from 4.6 to 4.8.

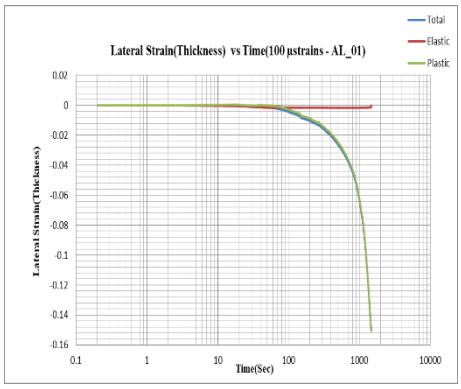

Fig. 4.5. Lateral Strain (thickness) vs Time

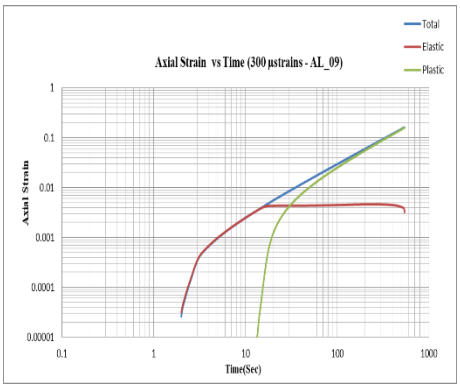

Fig. 4.6 Axial Strain vs Time

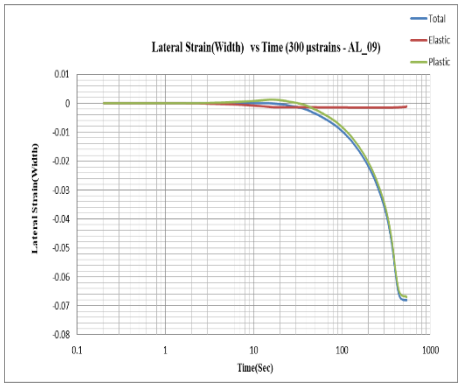

Fig. 4.7 Lateral Strain (width) vs Time

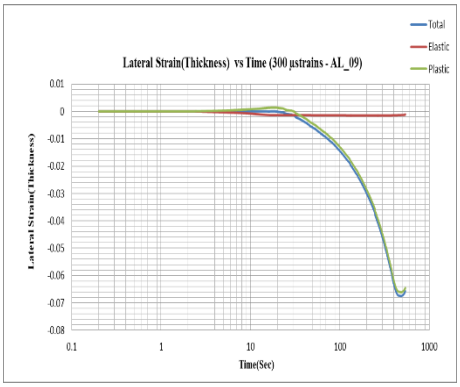

Fig. 4.8. Lateral Strain (thickness) vs Time

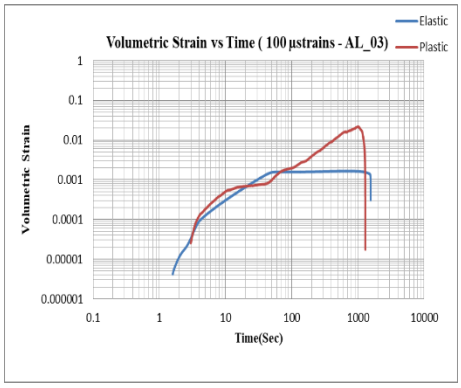

Fig. 4.9. Behaviour of volumetric strain vs Time

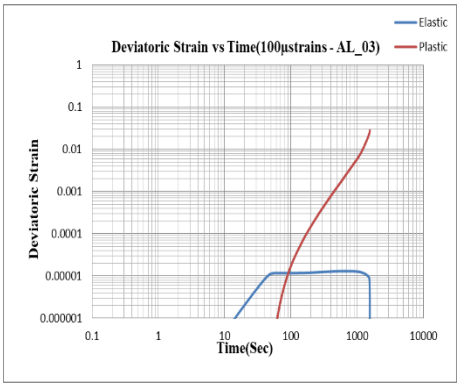

Fig. 4.10. Behaviour of Deviatoric strain vs Time

Volumetric strains and deviatoric strains, both elastic and plastic are computed for all the strain rates ranging from 100 µstrains to 1700 µstrains for all the aluminium specimens (AL_01 to AL_25). Also volumetric elastic and

plastic strain rates and deviatoric elastic and plastic strain rates were computed for all the strain rates ranging from 100 µstrains to 1700 µstrains for all the aluminium specimens (AL_01 to AL_25). Volumetric $(plastic/elastic)_v$ and Deviatoric strains$(plastic/elastic)_d$ ratios were computed for all the strain rates ranging from 100 µstrains to 1700 µstrains for all the aluminium specimens (AL_01 to AL_25). The next series of graphs, Fig. 4.9, 4.10 shows the variation of volumetric strain and deviatoric strain with deformation for aluminium specimen at 100 µstrains. These figures indicates the contribution from the elastic and plastic parts. Elastic volumetric strain increases with deformation in the beginning for aluminium. After yielding, there is a very little change in the elastic volumetric strain which shows that material is compressible in the elastic region. As observed in Fig. 4.9 it is found that there is a very less stress contribution from plastic volumetric strain immediately after yielding begins. Similarly the above phenomenon occurs in case of elastic deviatoric strain as seen in the graphs, Fig. 4.10 for aluminium. These observations suggest slipping between grain boundaries occurring inside the material without contributing to any kind of elastic strain. Fig. 4.12 and Fig. 4.13 depicts, major contribution comes from plastic deviatoric strain which is almost 4-5 times more than plastic volumetric strain during large deformation. The contribution from the elastic deviatoric strain during large deformation is almost constant. Their presence indicates the elastic unloading at any point in plastic range. Aluminium alloy shows that the deviatoric plastic strain rate is almost one order more than the corresponding volumetric plastic strain rate as indicated in graphs. Similarly the variation of volumetric strain and deviatoric strain with deformation for aluminium specimen at 700 µstrains are shown in the Fig. 4.11 and Fig. 4.12.

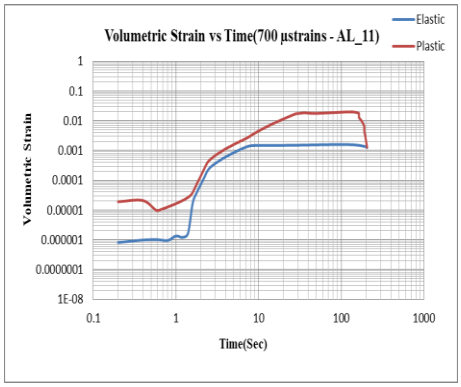

Fig. 4.11. Behaviour of volumetric strain vs Time

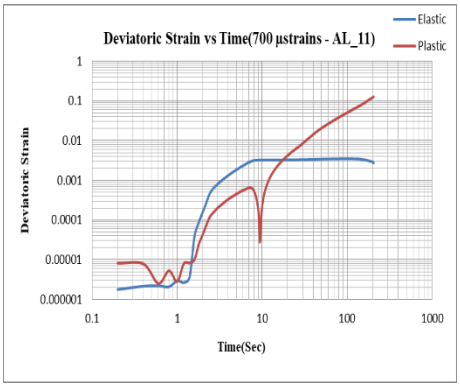

Fig. 4.12. Behaviour of Deviatoric strain vs Time

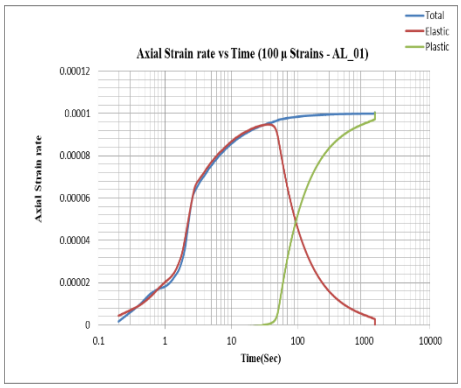

Fig. 4.13. Behaviour of Axial strain rate vs Time

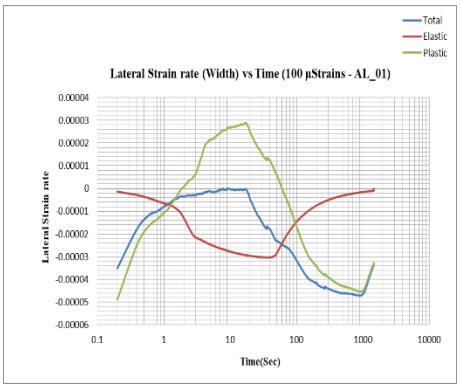

Fig. 4.14. Behaviour of Lateral rate (width) vs Time

The graphs of axial strain rate along length and lateral strain rates along width and thickness versus time are shown in Fig. 4.13, 4.14, 4.15 for aluminium specimen at 100 µstrains. All these graphs indicates that the major deformation comes from plastic strain rate. The next series of graphs, Fig. 4.16, 4.17 shows the variation of volumetric strain rate and deviatoric strain rate with deformation for aluminium specimen at 700 µstrains. The plastic strain rates are very small in the beginning of the deformation but increases rapidly around yielding though their initial behaviour is same. The rate of volumetric plastic strain rate is around one order less than the deviatoric plastic strain rate. This indicates the slipping of grain boundaries in shear during yielding due to sudden increase in plastic strain rate. After yielding, the plastic strain rates decreases. As observed in graphs, the volumetric plastic strain rate and devaitoric plastic strain rates are almost zero initially but increases rapidly on the onset of yielding. However after yielding, the plastic strain rates show a decreasing trend. In aluminium also, the rate of volumetric plastic strain rate is around one order less than the deviatoric plastic strain rate. Similarly the variation of volumetric strain rate and deviatoric strain rate with deformation for aluminium specimen at 1000 µstrains are shown in Fig. 4.18 and 4.19.

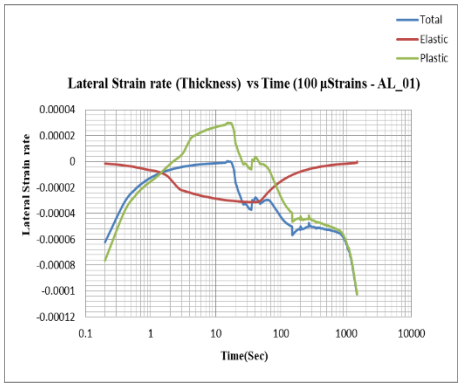

Fig. 4.15. Behaviour of Lateral strain rate (thickness) vs Time

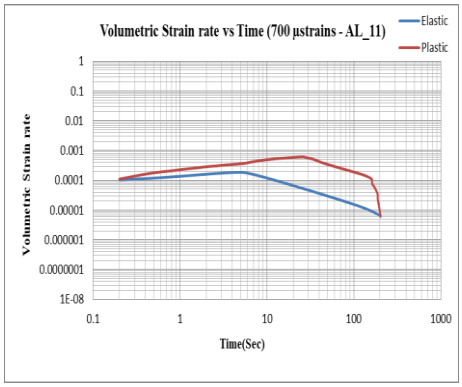

Fig. 4.16. Behaviour of volumetric strain rate vs Time

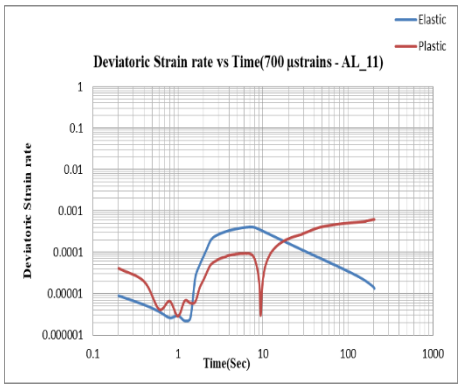

Fig. 4.17. Behaviour of Deviatoric strain rate vs Time

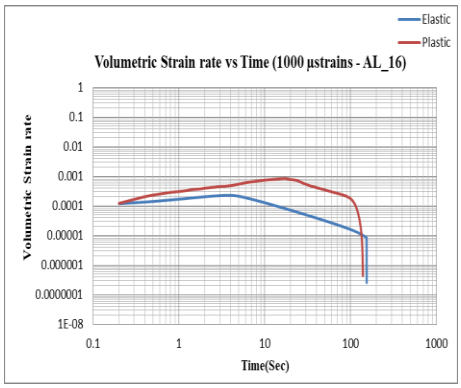

Fig. 4.18. Behaviour of volumetric strain rate vs Time

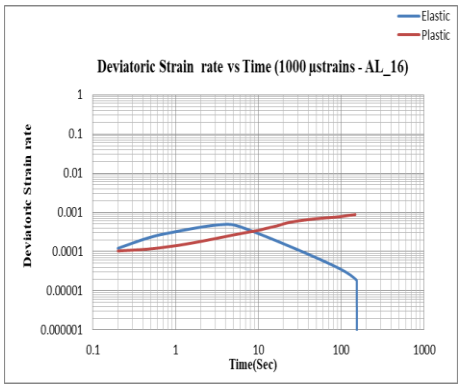

Fig. 4.19. Behaviour of Deviatoric strain rate vs Time

Table 6.13: Calculated material constants for Commercially available aluminium alloy

Constants	Aluminium
Bulk Modulus, K (GPa)	67.43
Shear Modulus, G (GPa)	26.72
Bulk Viscosity, µ' (MPa-s)	57
Shear Visocity, µ (MPa-s)	17

5. Conclusions

The calculated values of these eight material constants for commercially available aluminium specimen are tabulated in Table 6.13. From Table 6.13, it is found that the bulk viscosity for a material is more than the shear viscosity. The experimental behaviour, observations and data analysis reveals the change in plastic volume along with elastic volume change. The use of concept like activation energy in separating the elastic strain and plastic strain, plastic flow, etc. have a better physical insight than the classical yield theories. The major contribution during plastic flow comes from the plastic strain and the plastic stress hardly contributes anything to the total stress. The major part of the work done during deformation is due to the elastic stress than due to plastic stress.

6. List of References

[1] Andrade, E.N. da C., 1947. Viscosity and Plasticity. Heffer, Cambridge.

[2] Anjaneyulu, P., 1999. Towards elasto-plastic modelling using modified Navier-Stokes equations. M.E. thesis, Department of Mechanical Engineering, Indian Institute of Science, Bangalore.

[3] Astarita, G., 1990. The engineering reality of the yield stress. Journal of Rheology 34, 275.
[4] ASTM D785-03, 2005. Standard test method for Rockwell hardness of plastics and electrical insulating materials. Annual book of ASTM standards.
[5] ASTM E8-04, 2005. Standard test methods for tension testing of metallic materials. Annual book of ASTM standards.
[7] ASTM E34-94, 2005. Standard test methods for chemical analysis of aluminium and aluminium-base alloys. Annual book of ASTM standards.
[8] ASTM E132-04, 2005. Standard test method for Poisson's ratio at room temperature. Annual book of ASTM standards.
[9] ASTM E251-92, 2005. Standard test methods for performance characteristics of metallic bonded resistance strain gages. Annual book of ASTM standards.
[10] ASTM 1237-93, 2005. Standard guide for installing bonded resistance strain Gages. Annual book of ASTM standards.
[11] ASTM E1561-93, 2005. Standard practice for analysis of strain gage rosette data. Annual book of ASTM standards.
[12] Bari, S., Hassan, T., 2000. Anatomy of coupled constitutive models for ratcheting simulation. International Journal of Plasticity 16, 381.
[13] Bari, S., Hassan, T., 2001. Kinematic hardening rules in uncoupled modelling for multi-axial ratcheting simulation. International Journal of Plasticity 17, 885.
[14] Bari, S., Hassan, T., 2002. An advancement in cyclic plasticity modelling for Multi-axial ratcheting simulation. International Journal of Plasticity 18, 873.
[15] Barnes, H.A., Hutton, J.F., Walters, K., 1989. An Introduction to Rheology. Elsevier, Amsterdam.
[16] Barnes, H.A., 1999. The yield stress - a review or *παντα ρ ι*—everything flows? Journal of Non-Newtonian Fluid Mechanics 81, 133.
[17] Bingham, E.C., 1922. Fluidity and Plasticity. McGraw-Hill, New York.
[18] Bridgman, P.W., 1947. The effect of hydrostatic pressure on the fracture of brittle substances. Journal of Applied Physics 18, 246.
[19] Bridgman, P.W., 1952. Studies in large plastic flow and fracture with special emphasis on the effects of hydrostatic pressure. McGraw-Hill, New York.
[20] Bridgman, P.W., 1958. Physics of High Pressure. G. Bell & Sons, London.
[21] Chaboche, J.L., 1991. On some modifications of kinematic hardening to improve the description of ratchetting effects. International Journal of Plasticity 7,661.
[22] Chen, W.F., Han, D.J., 1988. Plasticity for Structural Engineers. Springer - Verlag, New York.
[23] Cheng, D.C-H., 1985. Yield stress: a time-dependent property and how to measure it. Report No. LR 540 (MH) Warren Spring Laboratory, Department of Industry, UK.
[24] Chiang, D.Y., Beck, J.L., 1996. Transformation method for implementing classical Multi-yield-surface theory using the hardening rule of Mroz. International Journal of Solids and Structures 33, 4239.
[25] Dafalias, Y.F., Popov, E. P., 1976. Rate-independent cyclic plasticity in a plastic internal variables formalism. Transaction of Mechanics Research Communications 3, 33.
[26] Dally, J.W., 1985. Experimental Stress Analysis. McGraw-Hill, Singapore.
[27] Dieter, G.E., 1988. Mechanical Metallurgy. McGraw-Hill , New York.
[28] Frost, H.J., Ashby, M.F., 1982. Deformation-Mechanics Maps. Pergamum Press, Oxford.
[29] Fung, Y.C., 1965. Foundation of Solid Mechanics. Englewood Cliffs, New Jersey.
[30] Gallagher *et al.*, Chichester: Wiley Inter science, 1, 25. Reference to non-Newtonian (plastic) fluids. Finite elements in fluids (eds),
[31] Gotoh, M., Yamashita, M., 2003. An aspect of plasticity with compressibility. International Journal of Plasticity 19, 383.
[32] Harrison, V.G.W.(Ed.), 1954. Rheology, Butterworth, London.
[33] Hill, R., 1950. Mathematical Theory of Plasticity. Oxford University Press, London.
[34] Hashiguchi, K., Tsutsumi, S., 2001. Elasto-plastic constitutive equation with tangential stress rate effect. International Journal of Plasticity 17, 117.
[35] Houwink, R., 1938. The yield value, second report on viscosity and plasticity. N.V. Noord - Hollandsche Uitgeversmaatschappij, Amsterdam.
[36] Jain, P., 2006. Measurements and simulation of elasto-plastic deformation. Msc thesis, Department of Mechanical Engineering, Indian Institute of Science, Bangalore.
[37] Karthikeyan, P., 2004. A new approach to process modelling and simulation of metal forming. M.Sc. thesis, Department of Mechanical Engineering, Indian Institute of Science, Bangalore.
[38] Kimball, A.L., Lovell, D.E., 1927. Internal friction in solids. Physical Review, 30, 948
[39] Kobayashi, H., Hiki, Y., Takahashi, H., 1996. An experimental study on the shear viscosity of solids. Journal of Applied Physics 80, 122.

[40] Jiang, Y., Sehitoglu, H., 1994a. Multi-axial cyclic ratchetting under multiple step loading. International Journal of Plasticity 10, 849.
[41] Jiang, Y., Sehitoglu, H., 1994b. Cyclic ratchetting of 1070 steel under multiaxial stress states. International Journal of Plasticity 10, 579.
[42] Khan, A.S., Huang, S., 1992. Experimental and theoretical study of mechanical behaviour of 1100 aluminium in the strain rate range 10^{-5} S^{-1} to 10^{-4} S^{-1}. International Journal of Plasticity 8, 397.
[43] Khan, A.S., Huang, S., 1995. Continuum Theory of Plasticity. John Wiley and sons, New York.
[44] Kimball, A.L., Lovell, D.E., 1927. Internal friction in solids. Physical Review, 30, 948.
[45] Lazan, B.J., 1968. Damping of Materials and Members in Structural mechanics. Oxford, Pergamon.
[46] Malvern, L.E., 1969. Introduction to Mechanics of Continuous Medium. Englewood Cliffs, New Jersey.
[47] Mroz, Z., 1967. On the description of anisotropic work-hardening. Journal of Mechanics and Physics of Solids 5, 163.
[48] Nadai, A., 1963. Theory of Flow and Fracture of Solids. McGraw-Hill, New York.
[49] Naghdi, P.M., 1958. An experimental study of initial and subsequent yield surfaces in plasticity. Journal of Applied Mechanics 25, 201.
[50] Ohno, N., Wang, J.D., 1993a. Kinematic hardening rules with critical state of dynamic recovery, part I: Formulation and basic features for ratchetting behaviour. International Journal of Plasticity 9, 375.
[51] Ohno, N., Wang J.D., 1993b. Kinematic hardening rules with critical state of dynamic recovery, part II: Application to experiments of ratchetting behaviour. International Journal of Plasticity 9, 375.
[52] Prager, W., 1961. Introduction to Mechanics of Continua. Boston, MA: Ginn.
[53] Rao, A.R., Shrinivasa, U., 2002. Towards simulation of elasto-plastic deformation: an investigation. Sadhana 27, 251.
[54] Rao, A.R., 2007. A unified constitutive model for large Elasto Plastic Deformation
[55] Rees, D.W.A., 1986. The sensitivity of strain gauges when used in the plastic range. International Journal of Plasticity 2, 295.
[56] Reiner, M., 1969. Deformation Strain and Flow. H.K. 3rd edition. Lewis, London.
[57] Saada, G., 2005. Hall-Petch revisited. Materials Science and Engineering A 400,146.
[58] Seth, B.R., 1970. Transition conditions. International Journal of Nonlinear Mechanics 5, 279.
[59] Shinde, K., 2004. Modeling of elsto-plastic deformation during sheet metal forming. M.E. thesis, Department of Mechanical Engineering, Indian Institute of Science, Bangalore.
[60] Sowerby, R., Uko, D.K., Tomita, Y., 1979. A review of certain aspects of the Bauschinger effect in metals. Materials Science and Engineering 41, 43.
[61] Stang, A.H., Greenspan, M., Newman, S. B., 1946. Poison's ratio of some structural alloys for large Strain. U.S. Department of Commerce National Bureau of Standard, research paper RP1742, 37, 211.
[62] Trouton, F.T., Andrews, E.S., 1903. On the viscosity of pitch-like substance. Physical Society 7, 346.
[63] Trouton, F.T., 1906. On the coefficient of viscous traction and its relation to that of viscosity. Philosophical Magazine A 77, 426.
[64] Valanis, K. C., 1971. A theory of visco-plasticity without a yield surface. Archives of Mechanics 23, 517.
[65] Valanis, K.C., 1980. Fundamental consequences of a new intrinsic time measure plasticity as a limit of the endochronic theory. Archives of Mechanics 32, 171.
[66] Valanis, K.C., Lee, C.F., 1981. Some recent developments of the endochronic theory with applications. Nuclear Engineering and Design 69, 327.
[67] Voyiadjis, G.Z., Thiagarajan, G., 1995. Anisotropic yield surface model for directionally reinforced metal-matrix composites. International Journal of Plasticity 11, 867.
[68] Watanabe, O., Atluri, S.N., 1986. Internal time, general internal varaible, and multi-yield-surface theories of plasticity and creep: a unification of concepts. International Journal of Plasticity 2, 37.
[69] Wegel, R.L., Walther, H., 1935. Internal dissipation in solids for small cyclic strains. Physics 6, 141.
[70] Wei, Y. J., Anand, L., 2004. Grain-boundary sliding and separation in polycrystalline metals: application to nanocrystalline fcc metals. Journal of the Mechanics and Physics of Solids 52, 2587.
[71] Wilson, C.D., 2002. A critical re-examination of classical metal plasticity. J. of Applied Mechanics 69, 63.
[**72] Zener, C., Hollomon, J.H.,** 1946. Problems in non- elastic deformation of metals. J. Appl. Phys. 17, 69-82.
[73] Zienkiewicz, O.C., Godbole, P.N., 1974. Flow of plastic and visco-plastic solids with special reference to extrusion and forming processes. International Journal of Numerical Methods in Engineering 8, 3.
[74] Zienkiewicz, O. C., Godbole, P.N., 1975. Viscous incompressible flow with special reference to non-Newtonian (plastic) fluids. Finite elements in fluids (eds), Gallagher et al., Chichester: Wiley Inter science, 1, 25.